DENSITY PROFILES OF SEMI-DILUTE POLYMER SOLUTIONS NEAR A HARD WALL: MONTE CARLO SIMULATION

WAN Y. SHIH, WEI-HENG SHIH and ILHAN A. AKSAY
Dept. of Materials Science and Engineering
University of Washington, Seattle, WA 98195

Introduction

A semi-dilute polymer solution is one in which polymers overlap. The bulk properties of semi-dilute polymer solutions have been studied extensively[1-3] and much has been known. The scaling theory has been very successful.[1,2] The predictions of the scaling theory about various physical quantities as a function of polymer concentration, c, have been confirmed experimentally.[1,3]

While the bulk properties of semi-dilute polymer solutions are well understood, the interfacial properties of a semi-dilute polymer solution are less well known. For example, the density profiles near a hard wall are difficult to examine experimentally. When a polymer solution is near a hard wall, it is thought that the polymer concentration is depleted in the proximity of the wall and the thickness of the depleted layer is on the order of the correlation length ξ. For semi-dilute polymer solutions in a good solvent, de Gennes predicts that the polymer concentration rises in a power-law fashion as $c(z) \sim (z/\xi)^m$, where z is the distance away from the wall and $m = 5/3$ [Refs. 2,4]. By arguing that the bulk osmotic pressure Π should be proportional to the first layer concentration $c(z=1)$, de Gennes predicts that in a lattice model, the concentration in the first layer near the wall behaves as $c(z = 1) \sim c^{9/4}$ [Ref. 2]. Though interfacial properties are technologically important, detailed study of polymer solutions near a wall, especially the determination of the concentration profiles, is experimentally difficult. The purpose of the present paper is therefore to use the Monte Carlo method[5] to simulate polymer solutions near a hard wall, to give a detailed account for the density profiles.

Model

We consider a $N_x \times N_y \times N_z$ cubic lattice in which there are M polymer chains each with N segments (monomers). A monomer is interacting with other monomers within the same chain (intra-chain) as well as in the other chains (inter-chain). In general, we consider for the monomer-monomer interaction (1) volume exclusion and (2) interactions up to the next nearest neighbors. Volume exclusion is taken into account by allowing no more than one monomer to occupy one lattice site. The nearest-neighbor interaction energy E_1 and the second-nearest-interaction E_2 can be positive, zero, or negative. One can control the values of E_1 and E_2 to simulate various solvent conditions. For instance, $E_1 = E_2 = 0$ represents an athermal polymer solution, which is the case we study in the present paper. Besides the monomer-monomer interactions, a monomer is also interacting with the hard walls on the top and at the bottom of the Monte Carlo cell. By hard wall we mean the wall is inpenetrable for the polymers. In addition to inpenetrability, we consider a nearest-neighbor wall-monomer interaction E_b, that is, when a monomer is right next to the wall, it gains energy E_b. In the present study, we consider $E_b = 0$. In the xy directions, we use the periodic boundary conditions.

Three types of movements are considered in the simulation. The first type of motion is the Brownian motion, namely, the polymer chains move as a whole in a random fashion as illustrated in Fig. 1a. The second type of motion is that a polymer can wiggle, specifically, a monomer in a chain can flip as illustrated in Fig. 1b. The third type of motion is reptation, that is, either end of a chain moves randomly to an adjacent unoccupied site and drags the rest of the chain along a *tube* that is shaped by its body as illustrated in Fig. 1c. Reptation is especially important when the density is high, so that the first two types of motions cannot effectively move the polymers. The motion of a polymer chain may be hindered by the presence of other polymers and/or by itself (that is, the motion of one part of a polymer

Mat. Res. Soc. Symp. Proc. Vol. 153. ©1989 Materials Research Society

chain can be hindered by another part of the chain). The hindrance of motion is correctly taken into account by the Boltzmann factor $e^{-\Delta E/T}$, where ΔE is the energy change due to the motion. Again, this is simulated with the standard Metropolis Monte Carlo method.

In all the simulations, for a given N, we choose Nx, Ny and Nz all at least larger than 8 R_G to ensure that the obtained R_G is not affected by the boundary conditions of the Monte Carlo cell. In each run, we discard 2000-6000 Monte Carlo steps and average over 5000-10000 Monte Carlo steps. For a given initial concentration $\varphi_{in} = MN/NxNyNz$, we perform 2-4 independent runs.

Results

Chains with $E_1 = E_2 = 0$ correspond to self-avoiding random walks and represent polymers in an athermal solution. In the Flory-Huggins's language, the χ parameter is zero in this case. We found that the double-logarithmic plot of the radius of gyration R_G of polymers with degree of polymerization N versus N (not shown) in the dilute regime has a slope 0.6, which agrees with the Flory's number ν which is 0.6 [Ref. 7] for athermal polymer solutions and is also within the numerical error of the self-avoiding random walks, which is .59 [Ref. 7].

One may define the segment density φ as the average occupancy of a lattice site by a segment (monomer). The segment density φ is related to the weight concentration c as $c = m\varphi/a^3$ where m is the molecular weight of a monomer and a is the segment length (lattice constant in the model). Throughout the text, we will use φ rather than c for convenience.

As one increases the segment density, at some point one passes from the dilute regime, where chains are well separated, to the semi-dilute regime, where chains overlap. An estimate of the crossover segment density φ^* from the dilute solution to the semi-dilute solution may be made by

$$\varphi^* = \frac{N}{\frac{4\pi}{3}R_G^3}, \tag{1}$$

where N is the number of segments in a chain or the degree of polymerization and R_G is the radii of gyration of the chains. Knowing the value for R_G from the simulations, one can calculate φ^*. For example, when $N = 40$, $R_G = 3.6$, therefore $\varphi^* = 0.2$; when $N = 100$, $R_G = 6.3$ and $\varphi^* = 0.095$.

Because of the overlapping of chains, a semi-dilute solution is very different from a dilute solution. For instance, for a given N, the radius of gyration R_G is independent of the segment density in dilute solutions but has φ dependence in the semi-dilute regime: $R_G^2/N \sim \varphi^{-1/4}$ [Ref. 1]. We show R_G^2/N versus the segment density φ in a double-logarithmic plot in Fig. 2 where full circles represent $N = 100$ and triangles represent $N = 40$. In both cases, R_G remains constant at low segment densities. At higher segment densities the two sets of data fall on one line with a slope -0.23, which is within the numerical error bars of the value $-\frac{1}{4}$ predicted by the scaling theory. Notice that R_G changes from dilute-solution behavior to semi-dilute-solution behavior at about the estimated crossover segment density φ^*, which is .095 for $N = 100$ and .2 for $N = 40$, as indicated by arrows in Fig. 2. In the following, we will focus on the density profiles near a wall in the semi-dilute regime where R_G^2/N shows the φ dependence.

Typical density profiles in the semi-dilute regime are shown in Fig. 3. Curve (a) is for $N = 40$ in a $35 \times 35 \times 50$ lattice with the bulk segment density $\varphi \sim 0.23$, and curve (b) is for $N = 100$ in a $50 \times 50 \times 70$ lattice with the bulk segment density $\varphi \sim 0.15$. The segment density is indeed smaller near the walls and rises monotonically toward the bulk value. The thickness of the depletion layer is on the order of the correlation length, as evidenced by the wider depletion layers in curve (b) where the correlation length ξ is larger than in curve (a), as is shown in more detail below. To look at the density profiles near the wall more closely, we show density profiles $\varphi(z)$ vs. z in a double-logarithmic plot for $N = 100$ in Fig. 4, where z is the distance away from the wall and $\varphi(z)$ is the segment density at distance z. The extrapolated slope at small z is (a) 1.23 for $\varphi = 1.35$, (b) 1.27 for $\varphi = .107$ and (c) 1.41

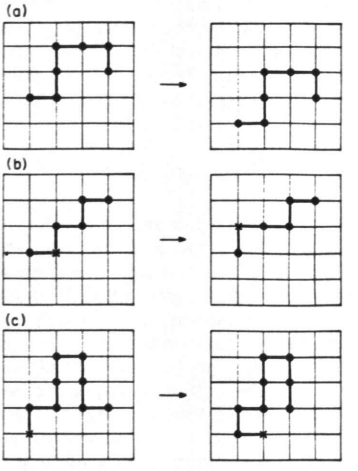

Fig. 1. (a) Brownian motion of the chain, (b) flipping of a monomer within a chain and (c) reptation of a chain.

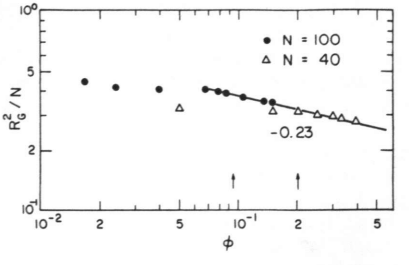

Fig. 2. R_G^2/N vs. φ for $N = 40$ (Δ) and for $N = 100$ ($\bullet$) where R_G and N are as defined in Fig. 3 and φ is the bulk segment density.

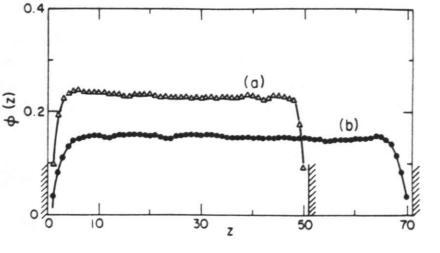

Fig. 3. Typical segment density profiles from $z = 1$ to N_z for (a) $N = 40$ with the bulk segment density $\varphi \sim 0.23$ and (b) $N = 100$ with the bulk segment density $\varphi \sim 0.15$. Notice that for profile (a) the walls are at $z = 0$ and $z = 51$ and for profile (b) the walls are at $z = 0$ and $z = 71$.

for $\varphi = .0925$, where φ is the bulk density. The extrapolated slope decreases with increasing bulk segment density and does not agree with the value 5/3 predicted by the scaling theory. The reason is that even with $N = 100$, the correlation length is still not large enough. In order to have the right extrapolated slope at small z one should have $z/\xi \ll 1$. Therefore, instead of extrapolating the exponent directly from the segment density profiles at small z, we use the following scaling form for the segment density profiles:

$$\varphi(z) = \varphi(1 - e^{-(\frac{z}{\xi})^m}) \tag{2}$$

where φ is the bulk segment density and ξ is the correlation length. This scaling function gives the right behavior both at small z and at large z. At small z/ξ, $\varphi(z)$ increases in a power law fashion with z: $\varphi(z) \sim (z/\xi)^m$ and at $z/\xi \gg 1$, $\varphi(z)$ gives the bulk density φ. We fit the three density profiles shown in Fig. 4 to the above form and the results are shown in Fig. 5. One can see that the fit is extremely good. Although the scaling function Eq. (2) fits well to the density profiles, we should mention that the choice of the scaling function is not unique as long as the function has the right behavior at small z and at large z. We choose the form Eq. (2) for the following reasons. (i) It is easy to plot and to extract the parameters m and ξ using Eq. (2). (ii) The exponential form is rather a natural choice for surface density profiles. For many systems, the interfacial density profiles are known to be exponential (hyperbolic tangential) except that the exponent m is unity in these systems while m may be different from unity for polymer solutions. From the lines in Fig. 5, we extract the exponent m which is the slope of the lines and the correlation length ξ, which is $e^{y_0/m}$, where y_0 is the intercept of the lines with the y axis. (a) $m = 1.64$, $\xi = 2.3$ for $\varphi = 0.135$; (b) $m = 1.61$, $\xi = 2.8$ for $\varphi = .107$; and (c) $m = 1.68$, $\xi = 3.2$ for $\varphi = .0925$. The extracted values of both m and ξ are very reasonable: (1) the values for m are in very good agreement with the value 5/3 predicted by the scaling theory and (2) the values for ξ show the right trend of decrease with increasing bulk concentration.

Throughout the whole semi-dilute density range we have simulated (up to $\varphi = 1.6$ for $N = 100$ and $\varphi = .32$ for $N = 40$), the scaling function Eq. (2) fits the segment density profiles remarkably well. For the exponent m, we always obtain values around 1.6 (ranging from 1.55 to 1.7). Although the segment density profiles are more complicated in the dilute regime, we also get very good fit if we just use the portion of the density profiles that are near the wall. An example is shown in curve (d) in Fig. 6, where we obtain $m = 1.63$ and $\xi = 5.9$. Thus, the segment density near the wall is proportional to $(z/\xi)^{5/3}$ in both dilute and semi-dilute solutions, except that $\varphi(z)$ increases monotonically in semi-dilute solutions but undergoes a maximum before reaching the bulk density value in dilute solutions. A more detailed account of the density profiles in the dilute regime will be published in a separate paper.

We show the extracted values of ξ versus the bulk segment density φ in a double-logarithmic plot in Fig. 6 where full circles and triangles represent $N = 100$ and $N = 40$ respectively. (1) ξ is independent of the segment density at low segment densities. Notice that the values of ξ at low segment densities are approximately equal to the values of the radii of gyration $R_G \sim 6.3$ for $N = 100$ and ~ 3.6 for $N = 40$, which is in agreement with the notion that in the dilute regime, the polymers are well separated and the correlation length is equal to the radius of the gyration of the chains. (2) When the segment density reaches the crossover density φ^*, the estimated values for $N = 100$ and for $N = 40$ are indicated by arrows in Fig. 6. The two sets of data fall on one line with a slope ~ -0.75, in agreement with the scaling prediction that the correlation length ξ in the semi-dilute regime depends only on the segment density and behaves as $\xi \sim \varphi^{-3/4}$. The effect of N is to change the value of the crossover segment density φ^*. In view of the remarkable result for the correlation length ξ obtained from the segment density profiles near a wall, this may turn out an easier way of calculating the correlation length. Normally, the correlation length is obtained from calculating the density-density correlation function, which is very time-consuming.

In Fig. 7 we plot φ_1 vs. φ where φ_1 is the segment density at $z = 1$ and φ is the bulk

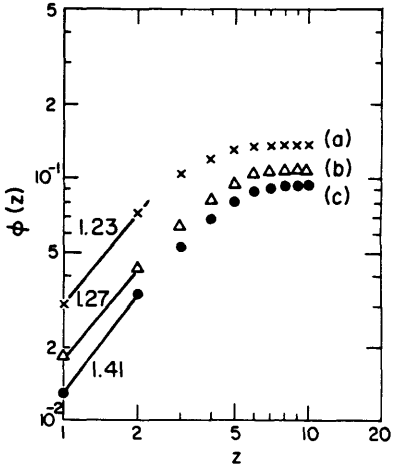

Fig. 4. The close-up of the segment density profiles for $N = 100$ near the wall (a) $\varphi = 0.135$, (b) $\varphi = 0.107$ and (c) $\varphi = 0.0925$, where φ is the bulk segment density.

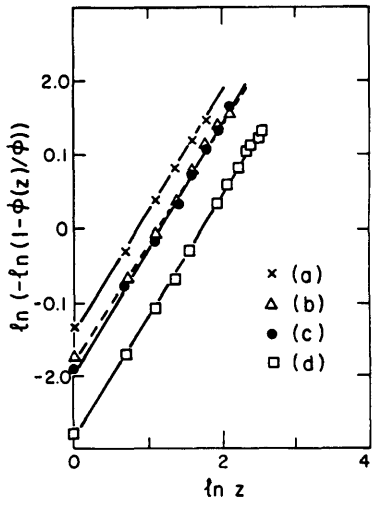

Fig. 5. $\ln\{-\ln[1-\varphi(z)/\varphi]\}$ vs. $\ln z$. The fitted values for the exponent m and the correlation length ξ are (a) $m = 1.64$, $\xi = 2.3$ for $\varphi = 0.135$, (b) $m = 1.61$, $\xi = 2.8$ for $\varphi = 0.107$, (c) $m = 1.68$, $\xi = 3.2$ for $\varphi = 0.0925$, (d) $m = 1.63$, $\xi = 5.9$ for $\varphi = 0.0167$.

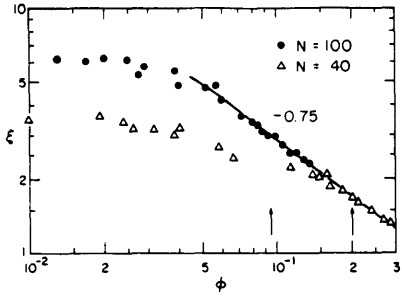

Fig. 6. ξ vs. φ for $N = 40$ (Δ) and for $N = 100$ ($\bullet$) where ξ is the correlation length and φ is the bulk segment density.

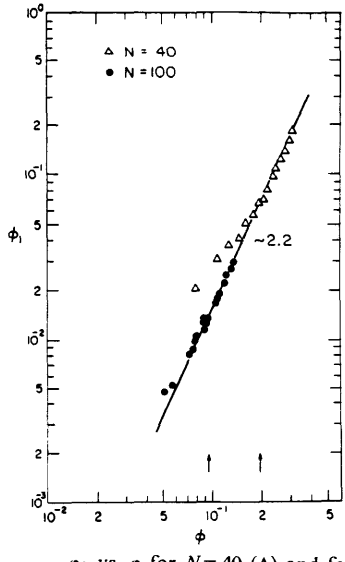

Fig. 7. φ_1 vs. φ for $N = 40$ (Δ) and for $N = 100$ ($\bullet$) where φ_1 is the first-layer segment density near the wall and φ is the bulk segment density.

segment density, as represented by the plateau in Fig. 4, for the semi-dilute regime. Again, full circles represent $N=100$ and triangles represent $N=40$. Again, the estimated crossover segment density $\varphi^* = .095$ for $N=100$ and $\varphi^* = .2$ for $N=40$ are indicated by arrows. One can see that above the crossover segment densities, the two sets of data fall on one line with a slope ~ 2.2, indicating that the behavior of the first-layer segment density is indeed similar to that of the bulk osmotic pressure Π, which behaves as $\Pi \sim \varphi^{9/4}$.

Summary

We have simulated semi-dilute athermal polymer solutions near a hard wall using the Monte Carlo method. We consider three types of polymer movements: (1) Brownian motion of a chain, (2) flipping of monomers, and (3) reptation. We have shown that in the semi-dilute regime, the radius of gyration R_G has φ dependence: $R_G^2/N \sim \varphi^{-0.23}$, in agreement with the scaling theory and also with the experiment. We have shown that in the semi-dilute regime, the segment density is depleted near the wall and the thickness of the depletion layer is on the order of the correlation length. By fitting the segment density profiles to the form Eq. (2), we are able to extract the exponent of the density profiles at small z/ξ, which ranges from 1.55 to 1.7, in agreement with 5/3 as predicted by the scaling theory. We have also extracted the correlation length which is also remarkably good: ξ is equal to the radius of gyration R_G at low densities and behaves as $\xi \sim \varphi^{-0.75}$ in the semi-dilute regime, again, in agreement with the scaling theory and also with the experiment. The first-layer segment density near the wall behaves as $\varphi_1 \sim \varphi^{2.2}$, indicating that the behavior of φ_1 is similar to that of the bulk osmotic pressure Π, which is known to behave as $\Pi \sim \varphi^{9/4}$. Therefore, for a hard wall, φ_1 is indeed proportional to the bulk osmotic pressure.

Acknowledgment

This work is supported by AFOSR and DARPA under Grant No. AFOSR-87-0114.

References

1. M. Daoud, J. P. Cotton, B. Farnoux, G. Jannink, G. Sarma, H. Benoit, R. Duplessix, C. Picot, and P. G. de Gennes, *Macromolecules*, **8**, 804 (1975).
2. P. G. de Gennes, ***Scaling Concepts in Polymer Physics***, (Cornell University Press, Ithaca, 1979), Chapter III and references cited therein.
3. K. Okano, E. Wada, Y. Taru, H. Hiramatsu, *Rep. Prog. Polym. Sci. Japan*, **17**, 141 (1974).
4. P. G. de Gennes, *Macromolecules*, **14**, 1637 (1981).
5. For a review, see ***Monte Carlo Methods in Statistical Physics***, (Springer-Verlag, Berlin-Heidelberg, 1986), ed. K. Binder, Chapter 1.
6. N. Metropolis, A. W. Rosenbluth, M. N. Rosenbluth, A. H. Teller, E. Teller, *J. Chem. Phys.*, **21**, 1087 (1953).
7. For a review, see Ref. 2 and the references therein.